Comparaison of temporal and frequency methods applied to ultrasonic nonlinear signals

Sonia Idjimarene, Mourad Bentahar, Rachid El Guerjouma, Marco Scalerandi

ACOUSTICS 2012

Comparaison of temporal and frequency methods applied to ultrasonic nonlinear signals

S. Idjimarene[a], M. Bentahar[a], M. Scalerandi[b] and R. El Guerjouma[a]

[a]Laboratoire d'acoustique de l'université du Maine, Bât. IAM - UFR Sciences Avenue Olivier Messiaen 72085 Le Mans Cedex 9
[b]DAST, Politecnico di torino, Corso Duca Degli Abruzzi 42, 10129 Torino, Italy
laum@univ-lemans.fr

Abstract

Extraction of the hysteritic nonlinear signature from an elastic wave propagating in a heterogeneous medium constitutes the main goal of researches in the nonlinear NDT field because of the large amount of possible applications (monitoring damage evolution, phase transitions, imaging of biological features,...). However, the presence of noise is a veritable issue in order to improve performances of the NDT techniques. In fact, nonlinear effects are ofen small and can easily be submerged within the noise.Thus, nonlinear analyses become difficult to set. Here, we analyse in detail the link between the amplitude threshold for detection of nonlinear effects and different kinds of noise, which might be present in experiments. We also discuss the efficiency of different approaches.

1 Introduction

Despite the huge potential for applications, the sensitivity of methods based on nonlinear elasticity to small/weak nonlinear features is strongly dependent on the signal-to-noise (SNR) ratio [1]. Thus, the nonlinear-to-linear ratio (NLR), defined as the ratio of the nonlinear signal over the linear one, is often smaller than the SNR and nonlinear effects are submerged into the noise level, even though recorded signals might be well above noise. In principle the problem could be overcome by increasing the amplitude A of excitation, since nonlinear effects increases as A^x, with $x > 1$ [2]. However, experimental limitations on amplification, frequency, transducers bandwidth, etc. always make it not practicable. Thus noise should always be considered to define the performance of a given experimental technique.

The present contribution aims to show the existence of strain amplitude thresholds for nonlinerity detection, which depend on the data analysis adopted. We will consider both environmental perturbations on the signal (assumed to be with amplitude not dependent on the driving) and noise related to the experimental set-up (i.e. proportional to the driving amplitude). Conclusions about the implications of our findings will also be discussed. In our analysis, we will use numerical data, obtained by using a model for the elastic wave propagation based on the Preisach-Mayergoytz approach [3, 4].

2 Theory

Techniques used in analysis to detect nonlinear contributions in the response of a sample to a given excitation, can be classified into three classes, depending on the nonlinear property exploited:

a) resonance frequency experiments exploit the dependence of the elastic constants on the amplitude of excitation, which leads to softening of materials when increasing strain levels. This feature can be monitored analysing the resulting shift of the resonance frequency to lower frequencies when increasing the driving. [5, 6];

b) experiments based on a frequency domain analysis are based on generation of higher harmonics during the propagation of an elastic wave. Such techniques are termed NonLinear Evolution Wave Spectroscopy methods (NEWS) [7, 8]

c) a time domain analysis can be performed when analysing the break of basic properties of linear elastic media, such as proportionality [9] and reciprocity [10]. These features are exploited by the Scaling Subtraction Method (SSM) [11] and Nonlinear Loss of Reciprocity based methods [12].

In our work, we adopted two of the above mentioned analysis methods: frequency domain analysis (FFT) and time domain analysis (SSM). The same experimental procedure can be adopted to measure signals used for the analysis. In fact, we could state that one excitation is applied to the sample and one response signal is measured. A proper time windowing is applied (at standing wave conditions) and the resulting signal is analysed in different ways in order to extract the measurement of a nonlinear physical quantity (y) which is measured at increasing driving amplitudes (x). Finally, from the relation between y and x, which is often a power law expression defined as:

$$y = (ax)^b \tag{1}$$

the coefficient a and the exponent b can be calculated. The two parameters give the strength of the nonlinearity (a) and the kind of nonlinearity (b), i.e. the physical nonlinear mechanisms involved. In this Section we will illustrate the procedure for the FFT and SSM methods of analysis. The excitation is assumed to be a continuum wave (cw) with frequency ω and amplitude A. Frequency is chosen close to the first resonance mode of the sample ($\omega = 25.9kHz$) to optimise excitation of the nonlinear feature, as done in experiments. Amplitude varies to give strain levels in the sample in the range $6 \cdot 10^{-9}$ to $7 \cdot 10^{-7}$, in agreement with experimental conditions. The amplitude span is of the order of 40dB. The temporal evolution of the velocity field is calculated, assuming a 1-D medium (length of 10 cm), with Young modulus $E = 72$GPa , density $\rho = 2700$ kg/m^3 and linear Q factor equal to 2000. A small scatterer is located in the center of the bar (in $x = 50$mm, with length $l = 0.5$mm). The intensity of the nonlinearity is varied by changing the nonlinearity density parameter λ.[13]

2.1 Time domain analysis: the Scaling Subtraction Method (SSM)

In the SSM analysis, one takes advantage of the influence of nonlinearity on the superposition principle. Indeed, once nonlinear effects are present, the proportionality between input and output is no longer valid [14]. Therefore, if we consider the response $u(t)$ of a system to an excitation of amplitude A, it is no longer equal to $A/A_0 \cdot u_0(t)$, where $u_0(t)$ is the response at a low amplitude excitation A_0. The procedure is thus to excite first the sample at a low amplitude (i.e. sufficiently low to provide negligible nonlinear effects) and

define a reference signal for amplitude A as:

$$u_{ref}(t) = A/A_0 \cdot u_0(t) \tag{2}$$

Afterwards, we introduce the nonlinear scaled subtracted signal (SSM signal)

$$w(t) = u(t) - u_{ref}(t) \tag{3}$$

Its energy (or amplitude) can be considered as the nonlinear variable to be calculated:

$$y_{SSM} = \frac{\sqrt{1/T \int_0^T w^2(t_0+t)dt}}{x_u} \tag{4}$$

where T is the time window length and t_0 the initial window time. Here x_u is the energy of the time signal recorded at amplitude A:

$$x_u = \sqrt{1/T \int_0^T u^2(t_0+t)dt} \tag{5}$$

This procedure is illustrated in Fig.1. Let us consider a temporal signal recorded at the receiver when a cw excitation (with frequency close to resonance) and amplitude A is applied. We select a short time window (in approximately standing wave conditions) and compare the signal $u(t)$ (solid black) with the reference signal built from Eq.1 using data simulated with a low excitation amplitude (dashed blue): see Fig.1a. The SSM signal (Eq. 3) is shown in Fig. 1b. Its

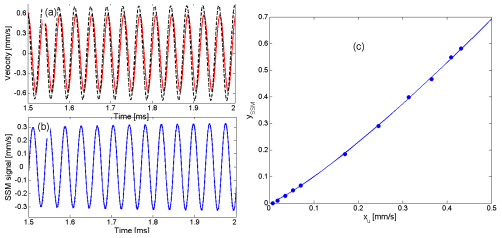

Figure 1: a) time signal for the large amplitude excitation (solid black) and reference signal (blue dotted line) b)SSM signal c)SSM indicator of nonlinearity

energy $y_{SSM}(A)$ can be estimated, together with the energy of the recorded signal: $x_u(A)$. The procedure is repeated for several amplitudes and y_{SSM} vs. x_u is reported in Fig.1c. The solid line represents the fitting with a power law expression (here $a_{SSM} = 0.037$ s/mm and $b_{SSM} = 1.21$).

2.2 Nonlinear Elastic Wave Spectroscopy analysis: Fast Fourier Transform (FFT)

The very same data set used for the SSM analysis can be analysed in the frequency domain. In this case, the generation of higher harmonics is exploited as indicator of nonlinearity. First, the signal $u(t)$ is filtered with a band-pass filter around the third harmonic obtaining a signal $u_{III}(t)$. The nonlinear variable which can be extracted is the energy of the filtered signal:

$$y_{FFT} = \frac{\sqrt{1/T \int_0^T u_{III}^2(t_0+t)dt}}{x_u} \tag{6}$$

where T is the time window length and t_0 the initial window time. Here x_u is again the energy of the time signal recorded at amplitude A (see Eq. 5).

The procedure is illustrated in Fig.2, where the same temporal signal as in Fig.1a ($u(t)$) is considered (cw excitation with frequency close to resonance, windowing in standing wave conditions).

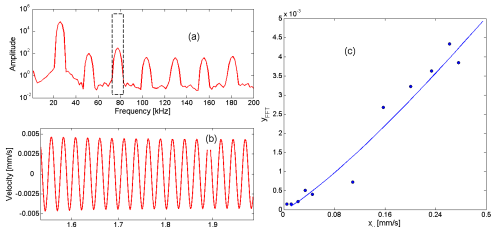

Figure 2: a)FFT of the output signal. b)Time signal corresponding to the third harmonic c)FFT indicator of nonlinearity

The FFT of the signal is reported in Fig. 2a, where evidence of third harmonics generation is clear. The band-pass filter range to obtain the u_{III} signal is highlighted in the figure (10kHz around the third harmonic). The resulting filtered signal is shown in Fig.2b. From here (at each amplitude) the energy of the filtered signal can be calculated using Eq. 6. Finally, y_{FFT} is plotted vs. x_u in Fig. 2c. The solid line represents the fitting with a power law expression (here $a_{FFT} = 6 \cdot 10^{-5}$[s/mm] and $b_{FFT} = 1.20$).

2.3 Discussion

Results presented in Fig.s 1b and 2b indicate a stronger nonlinear-to-linear noise ratio when the analysis is performed in the time domain (SSM). Indeed, the nonlinear signal (Fig.1b) is much higher than the nonlinear signal u_{III} (Fig.2b). For the given driving amplitude, the ratio is of about 100 (about 40dB), with obvious advantage for the analysis from the experimental point of view. This was indeed to be expected, since the analysis in the time domain also accounts for nonlinear effects occurring at the fundamental frequency, which are cancelled in the FFT analysis. It is remarkable that such effects are dominant, with respect to energy transferred into harmonics, thus suggesting that filtering around the fundamental frequency might be beneficial to improve the Non-Linear Signal to Noise ratio (NL-SNR). In Fig. 3a, y_{SSM} is plotted vs. x_u for different values of the hysteretic parameter λ (the larger λ the stronger the nonlinearity). Here and in the following we have used $\lambda = [4 \times 10^{-5}, 1.6 \times 10^{-4}, 4 \times 10^{-3}]Pa^{-2}$. In the plot, in log-log scale, data correspond to roughly parallel lines, thus indicating approximately the same exponent b for each λ . On the contrary, the coefficient a increases with increasing nonlinearity. It can be noticed that on the full range of excitation amplitudes used in the simulation, data fit a straight line.

In Fig. 3b, y_{FFT} is plotted vs x_u for two values of the hysteretic parameter, $\lambda = [1.6 \times 10^{-4}, 4 \times 10^{-3}]Pa^{-2}$. In the plot,

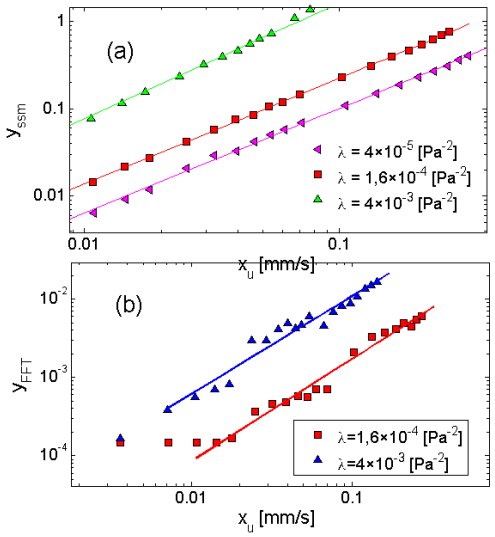

Figure 3: nonlinear quantity y vs. driving amplitude x_u for different nonlinearity strengths (λ). (a) SSM analysis ; (b) FFT analysis

in log-log scale, data for large driving amplitudes are distributed along almost parallel lines (solid lines represent the power law fitting), thus indicating approximately the same exponent b for each λ. Again, the coefficient a increases with increasing nonlinearity. However, for the lawer value of λ (not reported in the figure), the existance of a threshold for nonlinearity detection makes impossible the analysis of the data. Indeed, for small nonlinearity, y_{FFT} is almost constant for most of the excitation amplitudes . Third harmonics proportional to driving are generated indipendently from nonlinear effects due to material properties. These effects will be more important when noise is present.

3 Effects of experimental noise

As mentioned in the Introduction, the goal of the present paper is to analyse the effects of experimental noise in the detection of nonlinearity and in particular how the noise level influences the amplitude below which nonlinearity cannot be detected. We will consider here the combination of two noises. We consider an ambient noise n_a, which is at constant amplitude: it is defined as an additive stochastic variable (white noise) with zero average. Its strength η_a is measured in mm/s, and defined as the noise maximum amplitude. The equipment noise n_e has amplitude proportional to the driving. Thus, we define it as an additive stochastic white noise n_e, with strength η_e (adimensional).

The analysis in this Section is performed as in the previous one for the two methods, using signals perturbed as:

$$u'(t) = u(t) + n_a(t) + n_e(t)\max[u(t)] \quad (7)$$

3.1 Effects of equipment noise

For the analysis performed in the following, some preliminary discussion about the noise level on the nonlinear components of the signal is needed. The noise in the SSM signal w is given as a sum of two noises (see Eq.3), which effects both the large amplitude and the reference signals. Thus, the strength of the actual noise is to be properly rescaled. Given two identical white noises with autocorrelations ψ, the autocorrelation of the noise resulting from the sum of the two is $\sqrt{2}\Psi$. Thus, the actual noise in the SSM signal has strength $\eta_e^{SSM} = \sqrt{2}\cdot\eta_e$. On the contrary, the signal strength on the filtered signal u_{III} is much smaller than η_e, since the noise is band-pass filtered as well. For the case considered here, the noise on the filtered signal has strength $\eta_e^{FFT} \sim 0.04\cdot\eta_e$ (obtained analysing the filtering of an additive white noise variable in a 10kHz frequency window, the same used in our FFT analysis of data).

In experiments, equipment noise is of the order of a few percent of the signal, which corresponds to noise levels from -50 dB to -30 dB. For SSM, for reasons discussed in the next Subsection, we extend the analysis up to -20dB equipment noise. In Fig.4, the SSM and FFT results (Figs. 4(a)and 4(b) respectively) are shown for different equipment noise levels n_e for $\lambda = 1.6\cdot10^{-4}$. Curves can be fitted with in-

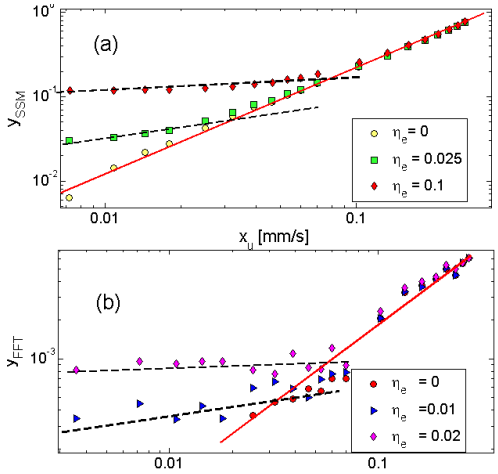

Figure 4: nonlinear quantity y vs. driving amplitude x_u for different strength n_e of the equipment noise. (a) SSM analysis; (b) FFT analysis

dependent power laws at low and high amplitudes . The detection threshold (intersection between the solid-red and dashed-black fitting lines) moves to higher amplitudes (on the x axes) when increasing noise. The analysis in the time domain is more stable. Indeed, up to a noise with maximum amplitude of the order of 10% of the signal amplitude (-20dB), we can still measure the nonlinear strength a and the exponent b, which are roughly independent from noise ($a_{SSM} = 0.07$s/mm; $b_{SSM} = 1.18$ for all curves).

Larger effects are present when the FFT analysis is performed. The white additive noise has a flat spectrum in the frequency domain, which is additive to the signal spectrum. Thus, considering the low values of the amplitude of the third harmonic (of the order of -40dB, maximum), they can be easily submerged into the noise spectrum. Thus the threshold is already very large at 1% of noise level (-40dB). However, once the nonlinear signal (the filtered signal u_{III} in this case) emerges from noise, the nonlinearity parameters are noise independent: $a_{FFT} = 0.002$s/mm; $b_{FFT} = 1.28$.

The threshold can be detected for each noise level and plotted as a function of $20\cdot Log(\eta_e)$ (see Fig.5). For all values of λ, the threshold increases exponentially, for both SSM and FFT analysis. The fitting function is drawn as a solid line in the plot (fitting coefficients are also reported in the plot).

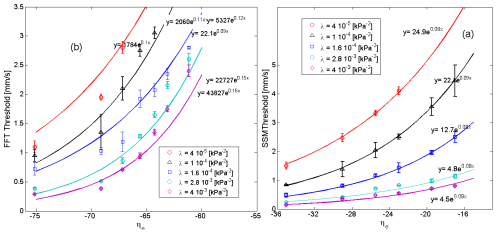

Figure 5: threshold for nonlinearity detection as a function of the equipment noise level (in dB). (a) SSM analysis; (b) FFT analysis

3.2 Effects of ambient noise

The effects of ambient noise on the threshold are much different in the SSM and FFT analysis.

For what concerns the former, we should consider that, for any given amplitude A, the ambient noise n_a in the w signal is amplified by a factor $k = A/A_0$, where A_0 is the lowest excitation amplitude (see Eq.3). Thus, in absence of equipment noise, the noisy SSM signal is:

$$w'(t) = w(t) + n_a(t) - kn_a(t) \tag{8}$$

In a first approximation

$$\begin{aligned} \max(u) &\propto A \\ \max(u_0) &\propto A_0 \end{aligned} \tag{9}$$

Thus

$$w'(t) = w(t) + n_a(t) - \frac{n_a(t)}{\max(u_0)} \max(u) \tag{10}$$

It follows that, neglecting $n_A(t)$, which is correct, except for small amplitudes, the ambient noise is equivalent to an equipment noise of intensity

$$n_e = \frac{\eta_a}{\sqrt{2}\max(u_0)} \tag{11}$$

where the factor $\sqrt{2}$ is due to neglecting $n_a(t)$ in Eq.10, while we have additivity of two identical noises in the w signal when equipment noise is present (in both the high amplitude and reference signals).

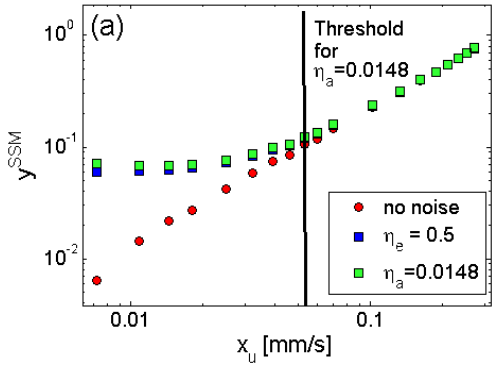

Figure 6: effects of an additive ambient noise $n_a(t)$ on SSM analysis

In Fig. 6, y_{SSM} is plotted vs. x_u for $\lambda = 1.6 \times 10^{-4}$ for $n_a = 0.0148$ mm/s. It can be seen that,for amplitudes larger than the threshold amplitude, the ambient noise provides the same results as those obtained with an equipment noise of amplitude given by Eq.11. At low amplitudes discrepancies are evident, given by non negligible effects of the term $n_a(t)$ in Eq. 10.

The situation is different in the case of the FFT analysis. Here, the ambient noise has the same strength for each excitation amplitude. Thus the signal to noise ratio is different for each amplitude A:

$$SNR_A = \frac{\eta_a}{\max[u]}$$

The ambient noise is significant only if it gives stronger effects than equipment noise at amplitudes larger than the detection threshold (defined in the following as Γ). When the driving amplitude is such that $x_u = \Gamma$, then $SNR_A \sim n_a/\sqrt{2}\Gamma$(we recall that $x_u$is the integral of $u^2(t)$, and $u(t)$is roughly sinusoidal). Thus, the condition for having effects on the threshold due to ambient noise is that:

$$n_a \geq \sqrt{2}\Gamma n_e \tag{12}$$

In Fig. 7, we consider $\lambda = 1.6\times10^{-4}$ and effect of ambient noise $n_a = 0.019$ mm/s on the FFT analysis. When each noise is considered separately,provided intensities are such to satisfy Eq. 12, we find the same threshold (approximately).

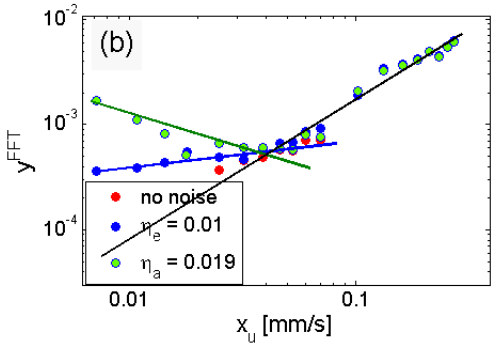

Figure 7: Effect of ambient noise on nonlinearity detection with FFT analysis

On the contrary, when both noises are present(see fig. 8), the threshold level is increased only when n_a is much larger. Otherwise (not reported) the threshold remains the same.

3.3 Discussion

The analysis reported in the previous Subsection indicates that:

- noise can hinder the presence of nonlinear features when the excitation amplitude is below a given threshold, which is much larger for FFT analysis, due to the lower NLR (nonlinear-to-linear signals ratio);
- ambient noise is always negligible in the case of FFT analysis, since its effect decreases with amplitude thus it becomes soon negligible with respect to equipment noise. An exception could perhaps be in the case of relaxation and conditioning measurements [15], which are always performed at low amplitude of excitation.

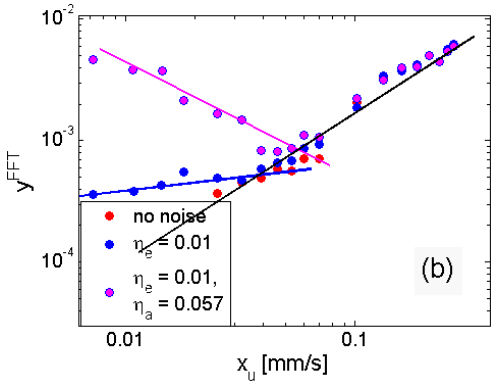

Figure 8: Effect of ambiant noise on the threshold of nonlinearity detection in presence of equipment noise

- ambient noise could be very important in the case of SSM analysis, especially when the lowest excitation amplitude is very small. In fact, the ambient noise is equivalent to an equipment noise with amplitude inversely proportional to the lowest excitation amplitude (see Eq.11). Thus, a difficulty of implementation for SSM analysis could be related to the choice of the amplitude of the lowest excitation A_0, which is as important as the largest excitation (in relation to the threshold). It is to be mentioned that the lower excitation level could not be increased arbitrarily, since it should be such that the elastic behavior is roughly linear. Increasing A_0 corresponds to including nonlinear features already in the reference signal, thus reducing the efficiency (NLR) of the method.

4 Conclusions

In the present paper we have tested the ability of both the Scaling Subtraction Method (SSM) and the Fourier analysis (FFT) to detect nonlinearity in an ultrasonic signal as a function of the excitation amplitude, both in the presence and absence of noise. We have considered the influence on the detection threshold of two kinds of noise we find in experiments (ambient and equipment noise). Numerical results indicate that the SSM is more sensitive to nonlinearity detection than FFT. In fact, the SSM indicator plot doesn't present any threshold of detection when noise is absent, while the FFT is unable to detect nonlinearity at very low excitation amplitudes or very low non linearity. Experimental data support our considerations[13].

Introducing the equipment noise (i.e. with strength proportional to the excitation amplitude), the FFT threshold of detection goes up and exceeding a given limit value of the noise amplitude, the method becomes completely not reliable, whereas the SSM method remains sensitive up to a larger value of noise (see Fig.s 4(a) and 4(b)). We also showed that adding an ambient noise is equivalent to introduce an equipement noise with strength given by Eq. 11 for the SSM procedure. Ambient noise becomes more and more important with decreasing the low amplitude excitation used in SSM. For the FFT method, the effects of ambient noise become soon not significant compared with the equipement noise. As a result, the threshold of detection is generally not modified.

References

[1] C.R.P. Courtney et al., J. of Sound and Vibration **329**, 4279 (2010).

[2] R.A. Guyer and P.A. Johnson, Physics Today **52**, 30-36 (1999).

[3] J.A. TenCate et al., Phys. Rev. Lett. **85**, 1024 (2000).

[4] P.P. Delsanto and M. Scalerandi, Phys.Rev.**B68**, 064107 (2003).

[5] K.Van den Abeele et al., NDT&E International **34**, 239-241 (2001).

[6] M. Bentahar, H. El Aqra, R. El Guerjouma, M. Griffa and M. Scalerandi, Phys. Rev. **B73**, 014116 (2006).

[7] K.Van den Abeele, P.A. Johnson and A. Sutin, Res. Nondestruct. Eval. **12**, 17 (2000).

[8] C. Payan, V. Garnier and J. Moysan, Cem. Concr. Res. **40**, 473-476 (2010).

[9] M. Scalerandi et al., Appl. Phys. Lett. **92**, 101912 (2008).

[10] J.A. Porto, R. Carminati and J.J. Greffet, J. Appl. Phys. **88**, 4845-4850 (2000).

[11] C.L.E. Bruno et al., Phys. Rev. **B79**, 064108 (2009).

[12] M. Scalerandi, A.S. Gliozzi and C.L.E. Bruno, J. Acoust. Soc. Am. **131**, EL81-EL85 (2012).

[13] M.Bentahar, R.El Guerjouma, S.Idjimarene, M.Scalerandi, Submitted to J.Applied Physics(2012).

[14] M. Scalerandi, A.S. Gliozzi, C.L.E. Bruno and P. Antonaci, Phys. Rev. **B81**, 104114 (2010).

[15] A.S. Gliozzi, M. Scalerandi, P. Antonaci, C.L.E. Bruno, Applied Physics A **100**, 421-424 (2010).